Dalton Transactions

Dynamic Article Links

Cite this: DOI: 10.1039/c1dt10420a

www.rsc.org/dalton

PAPER

Tuning the spin-transition properties of pyrene-decorated 2,6-bispyrazolylpyridine based Fe(II) complexes†

Rodrigo González-Prieto,[a] Benoit Fleury,[a] Frank Schramm,[a] Giorgio Zoppellaro,[a,b] Rajadurai Chandrasekar,[a,c] Olaf Fuhr,[a] Sergei Lebedkin,[a] Manfred Kappes[a] and Mario Ruben*[a,d]

Received 14th March 2011, Accepted 11th May 2011
DOI: 10.1039/c1dt10420a

Two 2,6-bispyrazolylpyridine ligands (bpp) were functionalized with pyrene moieties through linkers of different lengths. In the ligand 2,6-di(1*H*-pyrazol-1-yl)-4-(pyren-1-yl)pyridine (**L1**) the pyrene group is directly connected to the bpp moiety *via* a C–C single bond, while in the ligand 4-(2,6-di(1*H*-pyrazol-1-yl)pyridin-4-yl)benzyl 4-(pyren-1-yl)butanoate (**L2**) it is separated by a benzyl ester group involving a flexible butanoic chain. Subsequent complexation of Fe(II) salts revealed dramatic the influence of the nature of the pyrene substitution on the spin-transition behaviour of the resulting complexes. Thus, compound $[Fe(\mathbf{L1})_2](ClO_4)_2$ (**1**) is blocked in its high spin state due to constraints caused by a strong intermolecular π–π stacking in its structure. On the other hand, the flexible chain of ligand **L2** in compounds $[Fe(\mathbf{L2})_2](ClO_4)_2$ (**2**) and $[Fe(\mathbf{L2})_2](BF_4)_2{\cdot}CH_3CN{\cdot}H_2O$ (**3**) prevents structural constraints allowing for reversible spin transitions. Temperature-dependent studies of the photophysical properties of compound **3** do not reveal any obvious correlation between the fluorescence of the pyrene group and the spin state of the spin transition core.

Introduction

Spin transition (ST) compounds displaying high transition temperatures ($T_{1/2}$), wide thermal hysteresis ($\Delta T_{1/2}$) and thermochromism have increasingly moved into the focus of scientific interest due to their potential applicability in molecular devices.[1] To develop applications, it is necessary to address the functionalization of these molecular complexes, *e.g.* towards facilitating their processing for device fabrication. This aim can be achieved by tailored chemical modification of the organic ligands prior to the metal complexation.

Herein we report on the synthesis, structure and magnetic properties of three iron(II) complexes of the $[Fe^{II}(bpp)_2]^{2+}$-type (bpp = 2,6-di(1*H*-pyrazol-1-yl)pyridine) bearing pyrene groups in the 4′-position of the pyridine moiety. Previously, several $[Fe^{II}(bpp)_2]^{2+}$ compounds were shown to display ST in the range of or above room temperature in the solid state.[2–6] On the other side, the processing of ST compounds into switchable nanostructures was recently achieved by self-assembly and soft-lithography techniques.[7] Furthermore, integration of metal complexes *via* pyrene groups onto single-walled carbon nanotubes (CNT) has been shown to lead to confined magnetic systems of high interest for supramolecular spintronic applications.[8]

The decoration of $[Fe^{II}(bpp)_2]^{2+}$ complexes with pyrene groups is a straightforward approach towards implementation and integration of ST compounds into functional device architectures *via* supramolecular π–π stacking interactions. In particular, the study of $[Fe^{II}(bpp)_2]^{2+}$ complexes in confined environments allows for better understanding of the ST mechanism at the molecular level. There, cooperativity is known to play a key role in the shape (abruptness and hysteresis) and temperature of the spin transition in the solid state. Consequently, supramolecular approaches (coordination polymers, hydrogen bonding, π–π stacking, *etc.*) have been applied to molecular ST modules, partially with the objective being to increase the magnitude of cooperativity and ST temperatures.[9–11] Increasingly, the question of ST cooperativity is also being studied for Fe(II) centres distributed randomly within a matrix or on a substrate. However, in order to understand *e.g.* hybrid ST materials based on pyrene-modified ST complexes and sp^2-carbon materials (such as graphenes and carbon nanotubes) the persistence of the ST in the pyrene-modified Fe(II) complexes themselves has to be verified.

[a]*Karlsruhe Institute of Technology (KIT), Institute of Nanotechnology, Hermann-von-Helmholtz-Platz 1, 76344, Eggenstein-Leopoldshafen, Germany*
[b]*Department of Molecular Biosciences, University of Oslo, PO Box 1041 Blindern, Oslo, NO-0316, Norway*
[c]*School of Chemistry, University of Hyderabad, Prof. C. R. Rao Road, Gachi Bowli, Hyderabad, 500 046, India*
[d]*Institut de Physique et Chimie des Matériaux de Strasbourg (IPCMS), 23 rue de Loess, BP34, 67034, Strasbourg cedex 2, France. E-mail: mario.ruben@kit.edu; Fax: +49 (0) 7247 82 8976; Tel: +49 7247 82 6781*

† Electronic supplementary information (ESI) available: NMR, ESI mass and IR spectra of ligands **L1** and **L2**, and compounds **1**, **2** and **3**. Emission spectra of **3** excited at 270 nm and normalized emission intensity of polycrystalline pyrene butyric acid as a function of the temperature. X-Ray crystallographic parameters of **1**. CCDC reference number 790319. For ESI and crystallographic data in CIF or other electronic format, see DOI: 10.1039/c1dt10420a

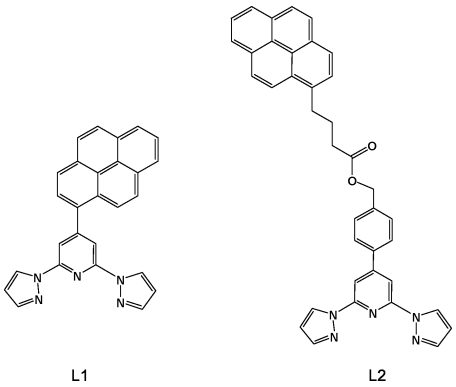

Scheme 1 Molecular structures of ligands **L1** and **L2**.

Guided by this motivation three different $[Fe^{II}(bpp)_2]^{2+}$ complexes have been prepared from two pyrene-substituted ligands, namely 2,6-di(1*H*-pyrazol-1-yl)-4-(pyren-1-yl)pyridine (**L1**) and 4-(2,6-di(1*H*-pyrazol-1-yl)pyridin-4-yl)benzyl 4-(pyren-1-yl)butanoate (**L2**) (Scheme 1). In **L1**, the pyrene moiety is directly coupled to the bpp ligand core, while in **L2**, the pyrene group is connected to the bpp core through a benzoyl ester group involving a butanoic acid linker. Thus, the pyrene part of the ligand is then clearly separated from the coordinating bpp unit by a flexible C_4 chain. Both ligands were then reacted in dichloromethane with methanolic solutions of iron(II) salts rendering the complexes $[Fe(\mathbf{L1})_2](ClO_4)_2$ (**1**), $[Fe(\mathbf{L2})_2](ClO_4)_2$ (**2**) and $[Fe(\mathbf{L2})_2](BF_4)_2{\cdot}CH_3CN{\cdot}H_2O$ (**3**).

Results and discussion

Synthesis

Ligand **L1** (2,6-di(1*H*-pyrazol-1-yl)-4-(pyren-1-yl)pyridine) was obtained as a white powder *via* a Suzuki cross-coupling reaction of 4′-iodo-2′,6′-dipyrazolyl-pyridine[12] with pyreneboronic acid. A Suzuki reaction between 4′-iodo-2′,6′-dipyrazolyl-pyridine and 4-(hydroxymethyl)phenylboronic acid was also used to synthesize 4-(4′-hydroxymethylphenyl)-2,6-bis(pyrazol-1-yl)pyridine. Esterification of pyrene butyric acid with this last compound yielded ligand **L2** (4-(2,6-di(1*H*-pyrazol-1-yl)pyridin-4-yl)benzyl 4-(pyren-1-yl)butanoate).

A methanolic solution of iron(II) perchlorate was layered over a dichloromethane solution of two equivalents of **L1**. Slow diffusion afforded dark yellow crystals of $[Fe(\mathbf{L1})_2](ClO_4)_2$ (**1**) with sufficient quality for single crystal analysis. In the case of **L2** the solid obtained after the reaction and later evaporation of the solvents is dissolved in acetonitrile, and diethyl ether was slowly diffused into this solution. The respective polycrystalline samples obtained yielded compounds $[Fe(\mathbf{L2})_2](ClO_4)_2$ (**2**), and $[Fe(\mathbf{L2})_2](BF_4)_2{\cdot}CH_3CN{\cdot}H_2O$ (**3**).

Solid state structure of compound 1

Single crystal X-ray diffraction studies show that compound **1** crystallizes in the *C*2/*c* space group with four $[Fe^{II}(\mathbf{L1})_2]^{2+}$ ions and eight perchlorate counter-anions per unit cell (Fig. 1). The $[Fe^{II}(\mathbf{L1})_2]^{2+}$ cation shows a twofold symmetry with the Fe1 atom lying on the crystallographic twofold axis. The crystal packing diagram reveals strong intermolecular π–π stacking (d = 3.38 Å) of adjacent inversion related pyrene units of neighbouring complexes (Fig. 1b and c) forming a 1-D chain-like structure. The Fe(II) ion is coordinated by two bpp ligands with Fe–N distances in the range 2.131(4)–2.202(4) Å. These bond distances clearly indicate the high-spin state (HS) of the iron(II) centre at 180 K. The coordination polyhedron around the iron(II) ion is strongly deviated from octahedral. This angular structural distortion is defined by the angle between the least squares planes formed by the two bpp ligands (θ = 68.9°) and the interligand angle N3′–Fe1–N3 (ϕ = 149.63(19)°).[5] Unfortunately, compounds **2** and **3**

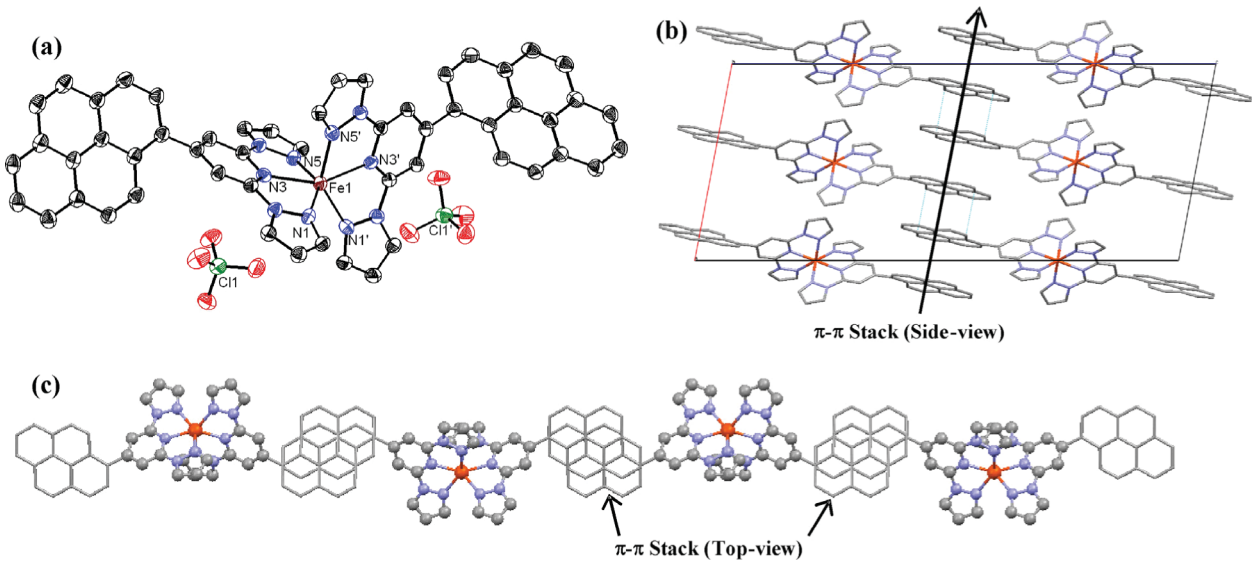

Fig. 1 **(a)** ORTEP view of compound **1** (30% probability ellipsoids, symmetry transformation: ′ ≡ $-x$, y, $\frac{1}{2} - z$) measured at 180 K. Selected bond lengths (Å): Fe1–N1 = 2.148(4), Fe1–N3 = 2.131(4), Fe1–N5 = 2.202(4). Selected bond angles (deg): N3′–Fe1–N3 = 149.63(19), N3–Fe1–N1′ = 130.42(13), N3–Fe1–N1 = 73.02(13), N3–Fe1–N5′ = 88.03(14), N3–Fe1–N5 = 71.78(13), N1′–Fe1–N1 = 94.3(2), N1–Fe1–N5 = 141.53(14), N1–Fe1–N5′ = 96.80(13), N(5′)–Fe(1)-N(5) = 97.00(18); hydrogen atoms are omitted for clarity. **(b)** Molecular packing revealing intermolecular π–π stacking. **(c)** Metallo-supramolecular 1D π–π stacked chain structure of the complex. In **(b)** and **(c)** the hydrogen atoms and counter ions are omitted for clarity.

did not provide crystals of sufficient quality for X-ray diffraction. However, they delivered satisfying analytical data in ESI-TOF MS, elemental analysis and ^{1}H NMR and FT-IR spectroscopies allowing the determination of their composition according to the formulas indicated above.

Temperature-dependent magnetic properties

Variable temperature magnetic measurements have been recorded for crystalline samples of compound **1** between 2 and 340 K, both for cooling and heating mode cycles (Fig. 2). The value of the $\chi_M T$ product is 3.46 cm^3 mol^{-1} K at 340 K which is close to the expected value for a HS ($S = 2$) state iron(II) ion. From 340 K down to ~50 K, the $\chi_M T$ value is nearly constant indicating the stable paramagnetic behaviour of the compound without any ST. Below 50 K, the $\chi_M T$ value suddenly decreased reaching a minimum value of 2.14 cm^3 mol^{-1} K at 2 K. This sudden decrease can be attributed to the zero-field splitting of the energy level of the Fe(II) HS ion in an octahedral environment. For compounds **2** and **3**, temperature-dependent magnetic measurements were performed using polycrystalline samples between 5 and 340 K – also for cooling and heating mode cycles. The temperature dependence of $\chi_M T$ of compound **2** showed a value of 3.41 cm^3 mol^{-1} K at 340 K which is very similar to the value shown by **1** and in the range of the usual values observed for [Fe$^{(II)}$(bpp)$_2$]-type compounds in the HS state.[6] Interestingly, in contrast to compound **1**, upon cooling below 300 K the $\chi_M T$ product sharply decreased and reached a value of 0.46 cm^3 mol^{-1} K at 90 K then remained nearly constant down to ~25 K. Below 25 K the magnetic moment reached a minimum value of 0.29 cm^3 mol^{-1} K at 5 K. The latter value is slightly too high to be attributed only to the Fe(II) LS ($S = 0$) state. Calculation of the number fraction (f) involved in the ST event shows that *ca.* 87% of the molecules undergo quite sharp ST, whereas the remaining *ca.* 13% of the molecules do not participate in the ST event. Moreover, the residual magnetic moment (0.29 cm^3 mol^{-1} K) at low temperature may include trace amounts of paramagnetic impurities. The ST temperature is centered at $T_{1/2}$ = 216 K. Similarly, compound **3** also shows a ST centered at 218 K although exhibiting a more abrupt transition and being almost complete with a $\chi_M T$ value of 0.09 cm^3 mol^{-1} K at 5 K. The $\chi_M T$ value at 340 K (3.18 cm^3 mol^{-1} K) is in the range of the values obtained for HS state iron(II) complexes.

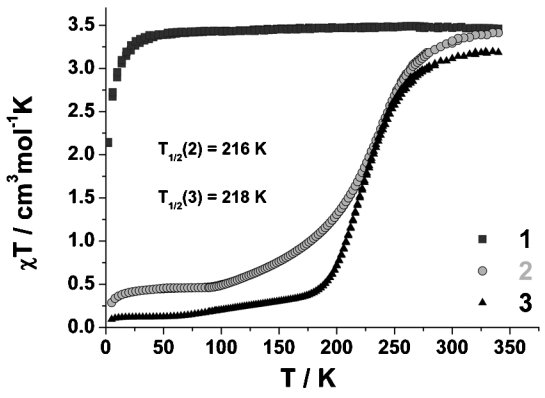

Fig. 2 The χ_T *vs* T plot of compounds **1**, **2**, and **3** cycled in the temperature range of 2–340 K with an applied magnetic field of 0.1 T.

In conclusion, the short linker compound **1** remains in the HS state at all temperatures probed while **2** and **3** exhibit reversible spin transitions between room-temperature and 90 K; regardless of the nature of counteranions used and the presence of crystal solvent molecules.

The difference in magnetic behaviour between compound **1** and compounds **2** and **3** can be understood by their structural differences. At first, the large π-system of the pyrene groups in compound **1** governs the overall supramolecular structure leading to strong intermolecular π–π stacking in the final lattice as demonstrated by the X-ray diffraction study. This effect forces the coordination sphere around Fe(II) to accommodate to this exterior constraint. In consequence, this molecular response leads to a highly distorted coordination octahedron as described above, favouring compound **1** to remain in the HS state over the whole temperature range. This has been previously observed in compounds showing similar distortions with $\theta < 76°$ and/or $\phi < 172°$ (ideally, 90 and 180°, respectively),[5] as well as in other spin transition compounds in which the systems are blocked in their HS state due to supramolecular constraints.[9f,11c] It has been well recognized that a change of the Fe–ligand bond distances by *ca.* 0.2 Å plays a key role in transmitting the elastic interaction between the ST sites in the solid state, leading ultimately to cooperative effects.[1b] Consequently, the peripheral π–π stacking interactions of the pyrene moieties prevent structural rearrangements at the coordination site. Thus, the formation of a more regular coordination environment, which is a requirement for the Fe(II) LS state, can not take place and the HS state prevails. Apparently, such a rearrangement would require too much energy to overcome the rigidity of the π–π stacking, and is therefore not possible at low temperature. A similar effect was also observed recently in another Fe(II) complex bearing sterically hindered bpp-type ligands and showing incomplete spin transition.[13] In this molecule, [PdCl(dpa)]$^+$ fragments on the 4-position of the bpp ligand form π–π and M···M intermolecular interactions leading to a supramolecular rigid organization of the molecules in the crystal lattice, trapping the compound kinetically in its high spin state at low temperatures.

Although the detailed molecular structure is still unknown for compounds **2** and **3**, the situation must be different owing to the increased flexibility of the pyrene linker in ligand **L2**. The absence of thermal hysteresis loops in their magnetic behaviour also demonstrates the lack of major cooperativity between molecules of these compounds in the solid state. Moreover, even if π–π stacking between adjacent pyrene groups can still occur, the flexible C_4 alkyl chain separator probably acts as a spring absorbing the constraint imposed by the π–π stacking. This effect attenuates the strain onto the coordination sphere around Fe(II) enabling the formation of a LS coordination sphere. Thus, ST is mediated by the more flexible ligand structure.

Temperature-dependent photoluminescence properties

In a recent publication, the group of Bousseksou and co-workers was able to observe spin state dependent emission quenching in rhodamine 110 doped [Fe^{II}(NH$_2$Trz)$_3$](tosyl)$_2$ nanoparticles (NH$_2$Trz = 4-amino-1,2,4-triazole).[14] To investigate the translation of this magneto-optical concept onto the (single-)molecular level, the correlation between the fluorescence of the pyrene group and

the respective iron(II) spin state was studied. The photoluminescence measurements were carried out on a polycrystalline sample of compound **3**, chosen due its relatively abrupt transition. The compound was found to be emissive (after excitation at 320 nm) over the full temperature range investigated (between 17 and 295 K). More specifically, the emission spectrum of compound **3** at 17 K comprises a structured band with vibronic peaks at 373 and 393 nm, as well as a broad band at around 460 nm tailing up to *ca.* 700 nm (Fig. 3). Both emissions originate from the pyrene groups and can be attributed to the "monomer" and "excimer" pyrene fluorescence, respectively.[15] This suggests that there are also close contacts between pyrene moieties in compound **3** (as found in the structural investigations for **1**) consequently allowing for the possibility of excimer formation.

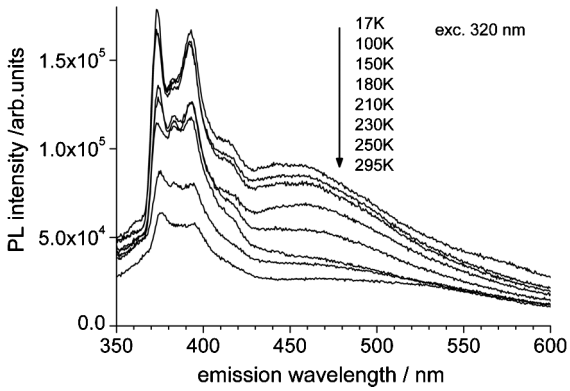

Fig. 3 Emission spectra of compound **3** (polycrystalline) excited at 320 nm at different temperatures. The half-bandwidths of the excitation and emission monochromators corresponded to 4 nm.

Another peculiar feature of the emission spectra of compound **3** is their notable dependence on the excitation wavelength as illustrated in a comparison of Fig. 3 and S19† (excitation wavelengths of 320 and 270 nm, respectively). For instance, the relative intensity of the "excimer" band is particularly large at an excitation wavelength of 270 nm and for temperatures below 150 K. However, it decreased strongly as the temperature increased. The whole spectrum then changes dramatically at ambient temperature (Fig. S20†). The origin of these spectral changes is not clear at the moment. There are also additional small emission peaks at ~326 and 357 nm (at 270 nm excitation).

Both the "monomer" and "excimer" emissions of pyrene groups in compound **3** do not show any specific correlation with the actual spin state of the complex core $[Fe^{II}(L_2)]^{2+}$. Measurements of the emission intensities above and below the spin transition temperature $T_{1/2}$ = 218 K reveal a rather continuous dependence on the temperature as illustrated in Fig. 4 for both emission wavelengths. The temperature dependence observed, which manifests a moderate increase of the emission intensity below ~200 K, seems to be typical for pyrene-based fluorophors. Correspondingly, a direct relationship with the spin state of **3**, can be ruled out by comparing with studies of analogous nonmagnetic compounds (*e.g.*, pyrene butyric acid, see Fig. S21†) which show the same moderate temperature dependency of the emission intensity as observed for **3**.

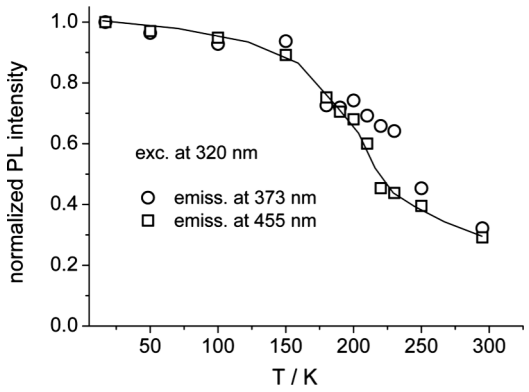

Fig. 4 Emission intensity of solid compound **3** as a function of the temperature. Wavelengths are 320 nm for excitation and 373 nm (monomer) and 455 nm (excimer) for emission. The solid line is drawn as a guide for eye.

Conclusion

Two spin transition complexes bearing flexible pyrene linkers were successfully designed and synthesized: $[Fe^{II}(\mathbf{L2})_2](ClO_4)_2$ (**2**) and $[Fe^{II}(\mathbf{L2})_2](BF_4)_2{\cdot}CH_3CN{\cdot}H_2O$ (**3**). Both complexes show very similar reversible spin transitions with transition temperatures of 216 and 218 K, respectively. In strong contrast, the analogous short-linker pyrene compound $[Fe^{II}(\mathbf{L1})_2](ClO_4)_2$ [**1**] does not show any spin transition and remains blocked in the HS state over the full temperature range investigated. In addition, no influence of the spin state on the fluorescence intensities was observed; moderate temperature-dependent fluorescence quenching was shown to be non-magnetic in nature by comparison to diamagnetic reference compounds. In conclusion, we have demonstrated the importance of the flexibility of the ligand around Fe(II) centres for balancing structural constraints which prevent the ST process from occurring and cooperativity. Functionalization of planar surfaces and non-planar CNTs with compounds **2** and **3**, as well as magnetic and electrical studies of the corresponding devices[17] and materials[18] are under investigation.

Experimental

General experimental methods

All reagents and solvents used in this study are commercially available and were used without any further purification, except when stated. 4′-Iodo-2′,6′-dipyrazolyl-pyridine was synthesized according to the reported procedure.[12]

^{1}H and ^{13}C NMR spectroscopic data were recorded on a Bruker DPX 300 and a Bruker Ultrashield plus 500 spectrometers with solvent-proton as internal standard. Mass data were acquired with a Voyager-DE PRO Bio spectrometry work station for MALDI-TOF and with a MicrOTOF-Q II Bruker for ESI-TOF. MALDI spectra were measured with no additional matrix compound other than the sample itself. Infrared spectra were recorded using KBr-pressed pellets with a Perkin-Elmer Spectrum GX FT-IR spectrometer. Elemental analyses were carried out on a Vario Micro Cube.

Magnetic susceptibility

Temperature-dependent static susceptibilities were recorded using an MPMS-5S (Quantum Design) SQUID magnetometer in a homogeneous 0.1 T external magnetic field. Gelatine capsules were used as sample containers. The very small diamagnetic contribution of the gelatine capsule had a negligible contribution to the overall magnetization, which was dominated by the sample. The diamagnetic corrections of the molar magnetic susceptibilities were applied using well-known Pascal's constants.

Measurements were recorded for crystalline samples of **1** and for polycrystalline samples of **2** and **3**.

Single crystal X-ray diffraction

X-Ray data collection was performed on a STOE IPDS II diffractometer with graphite monochromated Mo-Kα radiation at 180 K. Crystallographic and refinement data of **1** are summarized in a table in the ESI† (CCDC reference number 790319). Structure solution by direct methods and refinement with anisotropic temperature factors for all non-hydrogen atoms were carried out by using the SHELX program package.[16] H atoms were calculated on idealized positions.

Photoluminescence study

Photoluminescence (PL) measurements were performed on a Spex Fluorolog-3 spectrometer equipped with a 450 W xenon light source, double excitation and emission monochromators and a thermoelectrically cooled Hamamatsu R9910 photomultiplier as a detector. Solid samples (polycrystalline powders) were dispersed in viscous polyfluoroester (ABCR GmbH), layered between two 1 mm thick quartz plates and mounted on the cold finger of an optical closed-cycle cryostat (Leybold) operating at ~15–350 K. Emission was collected at an ~30° angle relative to the excitation light beam. All emission spectra are presented corrected for the wavelength-dependent response of the spectrometer and detector (in relative photon flux units).

Synthesis of 2,6-di(1*H*-pyrazol-1-yl)-4-(pyren-1-yl)pyridine (L1)

4′-Iodo-2′,6′-dipyrazolyl-pyridine (0.4643 g, 1.38 mmol), pyreneboronic acid (0.3390 g, 1.38 mmol) and $Pd(PPh_3)_4$ (0.1581 g, 0.14 mmol, 10%) were suspended in an Ar gas bubbled solution of 1,4-dioxane (150 mL) and 2 M Na_2CO_3 (10 mL) and heated to 70 °C for 5 days under an argon atmosphere. The 1,4-dioxane was removed using a rotary evaporator and the remaining residue was extracted twice with 100 mL of $CHCl_3$ and washed with water (2 × 200 mL). The separated organic layer was dried over $MgSO_4$ and the solvent was removed by evaporation. The solid orange residue was washed with methanol to remove the soluble impurities and to afford a yellowish coloured powder. The solid residue was column chromatographed on neutral alumina with ethyl acetate/hexane (1 : 4) as eluent. The second colourless fraction was collected and the resultant combined solution upon evaporation yielded a white powder of **L1** (0.350 g, yield 62%). **^{1}H NMR (500 MHz, $CDCl_3$, 25 °C, δ (ppm)):** 8.69 (d, 2H), 8.27–8.02 (m, 11H), 7.78 (d, 2H), 6.55 (m, 2H). **^{13}C NMR (125 MHz, $CDCl_3$, 25 °C, δ (ppm))**: 155.34, 150.31, 142.62, 134.02, 131.84, 131.49, 130.95, 128.68, 128.35, 128.30, 127.45, 127.43, 127.06, 126.38, 125.78, 125.52, 125.01, 124.87, 124.83, 124.31, 111.45, 108.21. **ESI-TOF MS** in $CHCl_3$ + formic acid (Da): *m*/*z* (rel. intensity, assigned structure) = 279.13 (8%, $C_{21}H_{13}N$, fragment); 412.21 (100%, $C_{27}H_{18}N_5$, **L1** + H^+, calc. = 412.16); 434.21 (5%, $C_{27}H_{17}N_5Na$, **L1** + Na^+); 823.42 (3%, $C_{54}H_{35}N_{10}$, **L1**$_2$ + H^+).

Synthesis of 4-(4′-hydroxymethylphenyl)-2,6-bis(pyrazol-1-yl)pyridine

4′-Iodo-2′,6′-dipyrazolyl-pyridine (2 g, 6 mmol), 4-(hydroxymethyl)phenylboronic acid (0.911 g, 6 mmol) and $Pd(PPh_3)_4$ (0.700 g, 0.6 mmol, 10%) were suspended in a N_2 gas bubbled solution of 1,4-dioxane (130 mL) and 2 M Na_2CO_3 (20 mL) and heated to 70 °C for 3 days under a nitrogen atmosphere. The 1,4-dioxane was removed using a rotary evaporator and the remaining residue was extracted twice with 100 mL of $CHCl_3$ and washed with water (3 × 200 mL). The separated organic layer was dried over $MgSO_4$ and the solvent was removed by evaporation. The obtained light brown solid was chromatographed on a silica column using ethyl acetate/hexane (7 : 3) as eluent until the first non-desired yellow fraction is eliminated. The second colourless fraction was collected eluting with ethyl acetate/ethanol (17 : 3) and, upon evaporation, the resultant combined solutions yielded a white solid of 4-(4′-hydroxymethylphenyl)-2,6-bis(pyrazol-1-yl)pyridine (1.4 g, yield 73%). **^{1}H NMR (300 MHz, $CDCl_3$, 25 °C, δ (ppm)):** 8.60 (d, 2H, pyrazole), 8.10 (d, 2H, pyridine), 7.78 (m, 4H), 7.48 (d, 2H, phenyl), 6.51 (m, 2H, pyrazole), 4.78 (s, 2H, –CH_2–), 2.26 (s, 1H, –OH). **^{13}C NMR (75 MHz, $CDCl_3$, 25 °C, δ (ppm)):** 153.83, 150.60, 142.73, 142.41, 136.53, 127.49, 127.40, 127.30, 108.02, 107.18, 64.75. **MALDI-TOF** (Da): *m*/*z* (rel. intensity, assigned structure) = 318.13 (100%, $C_{18}H_{16}N_5O$, M + H^+, calc. = 318.13); 617.07 (26%, $C_{36}H_{29}N_{10}O$, fragmentation + association); 635.08 (11%, $C_{36}H_{31}N_{10}O_2$, 2M + H^+).

Synthesis of 4-(2,6-di(1*H*-pyrazol-1-yl)pyridin-4-yl)benzyl 4-(pyren-1-yl)butanoate (L2)

4-(4′-Hydroxymethylphenyl)-2,6-bis(pyrazol-1-yl)pyridine (0.4301 g, 1.4 mmol), 1-pyrenebutyric acid (0.4040 g, 1.4 mmol), *N*,*N*′-dicyclohexylcarbodiimide (0.2835 g, 1.4 mmol) and dimethylaminopyridine in catalytic quantities were suspended in 150 mL of dry dichloromethane, and this reaction mixture was stirred for two days at room temperature under an inert atmosphere. After evaporation of solvents, the obtained solid was chromatographed on a silica column using ethyl acetate/hexane (1 : 1) as eluent. The white solid obtained after rotary evaporation of the first colourless fraction was washed with diethyl ether yielding **L2** (0.4847 g, yield 61%). **^{1}H NMR (300 MHz, $CDCl_3$, 25 °C, δ (ppm)):** 8.60 (d, 2H), 8.27 (d, 1H), {8.16–7.95 (m, 9H)}, 7.84 (d, 1H), 7.79 (d, 4H), 7.46 (d, 2H), 6,52 (m, 2H), 5,18 (s, 2H), 3,40 (t, 2H), 2.55 (t, 2H), 2.25 (m, 2H). **^{13}C NMR (125 MHz, $CDCl_3$, 25 °C, δ (ppm)):** 173.36, 153.70, 150.75, 142.53, 137.77, 137.40, 135.67, 131.51, 131.00, 130.11, 128.93, 128.87, 127.59, 127.56, 127.48, 127.36, 126.85, 125.96, 125.21, 125.09, 125.04, 124.93, 123.38, 108.14, 107.34, 65.78, 34.00, 32.85, 26.85. **ESI-TOF MS** in $CHCl_3$ + formic acid (Da): *m*/*z* (rel. intensity, assigned structure) = 588.32 (100%, $C_{38}H_{30}N_5O_2$, **L2** + H^+, calc. = 588.24); = 610.30 (24%, $C_{38}H_{29}N_5NaO_2$, **L2** + Na^+).

Synthesis of $[Fe(L1)_2](ClO_4)_2\cdot(H_2O)$ [1(H_2O)]

22.3 mg (0.054 mmol) of 2,6-di(1*H*-pyrazol-1-yl)-4-(pyren-1-yl)pyridine (**L1**) was dissolved in 7 mL of dichloromethane. 9.80 mg (0.027 mmol) of iron(II) perchlorate hydrate was dissolved in 2 mL of methanol and this solution was subsequently layered over the solution of **L1**. Slow diffusion affords complex **1** as dark yellow single crystals, which were suitable for single crystal X-ray diffraction (16.5 mg, yield 56%). **Elemental analysis found (calcd)** for $C_{54}H_{36}Cl_2FeN_{10}O_9$ {$[Fe(\mathbf{L1})_2](ClO_4)_2\cdot H_2O$, 1095.703 g mol^{-1}}: C 59.28 (59.20)%; H 3.29 (3.31)%, N 12.86 (12.78)%. **^{1}H NMR (500 MHz, CD_3CN, 25 °C, δ (ppm)):** 63.01 (s, pyrazole), 56.59 (s, pyridine), 37.90 (s, pyrazole), 36.32 (s, pyrazole), 8.46–7.88 (m, pyrene). **ESI-TOF MS** in CH_3CN (Da): *m*/*z* (rel. intensity, assigned structure) = 249.56 (6%, $FeC_{28}H_{21}N_5O$, M^{2+} – L1 + CH_3OH); 254.08 (8%, $FeC_{29}H_{20}N_6$, M^{2+} – L1 + CH_3CN); 263.09 (9%; $FeC_{29}H_{22}N_6O_2$, M^{2+} – L1 + CH_3CN + H_2O); 439.17 (100%, $FeC_{54}H_{34}N_{10}$, **M^{2+}**, calc. 439.12); 566.10 (12%, $FeC_{27}ClH_{17}N_5O_4$, M^{2+} – L1 + ClO_4^-); 644.76 (6%, $FeC_{81}H_{51}N_{15}$, M^{2+} + L1); 977.28 (9%, $FeC_{54}ClH_{34}N_{10}O_4$, M^{2+} + ClO_4^-). **FT-IR (KBr):** $\tilde{\nu}$/cm^{-1} = 3148, 3114, 3043, 1621, 1567, 1523, 1497, 1457, 1407, 1338, 1235, 1216, 1174, 1099, 1057, 1014, 975, 874, 842, 792, 765, 732, 720, 680, 665, 645, 622, 601, 502.

Synthesis of $[Fe(L2)_2](ClO_4)_2$ (2)

A solution of iron(II) perchlorate hydrate (15.25 mg, 0.042 mmol) in MeOH (3 mL) was added to 51.5 mg (0.088 mmol) of **L2** dissolved in CH_2Cl_2 (12 mL). Immediately, a colour change from colourless to yellow occurred and the reaction mixture was stirred at room temperature for two hours under a N_2 atmosphere. Solvent was removed by rotary evaporation, the resulting yellow-orange solid was dissolved in CH_3CN and diethyl ether was slowly diffused into this solution. The polycrystalline sample obtained contains acetonitrile and water as can be deduced from its elemental analysis. These solvents are slowly lost on exposure to air yielding, after a few weeks, the compound $[Fe(\mathbf{L2})_2](ClO_4)_2$ (**2**) (44.3 mg, yield 74%). **Elemental analysis found (calcd)** for $C_{76}H_{58}Cl_2FeN_{10}O_{12}$ {$[Fe(C_{38}H_{29}O_2N_5)_2](ClO_4)_2$, 1430.122 g mol^{-1}): C 63.67 (63.83)%; H 4.170 (4.09)%, N 9.80 (9.79)%. **^{1}H NMR (300 MHz, CD_3CN, 25 °C, δ (ppm)):** 66.69 (s, pyrazole), 58.42 (s, pyridine), 39.59 (s, pyrazole), 39.09 (s, pyrazole), 8.26–7.41 (m), 5.70 (s, –C<u>H</u>$_2$–Ph), 3.33 (t, –CH_2–), 2.50 (t, –CH_2–). **ESI-TOF MS** in CH_3CN (Da): *m*/*z* (rel. intensity, assigned structure) = 615.20 (100%, $FeC_{76}H_{58}N_{10}O_4$, **M^{2+}**, calc. = 615.20); 678.14 (30%, $FeC_{38}H_{29}N_5O_2Cl$, M^{2+} – L2 + Cl^-); 909.32 (16%, $FeC_{114}H_{87}N_{15}O_6$, M^{2+} + L2); 1202.94 (7%, $FeC_{152}H_{116}N_{20}O_8$, M^{2+} + 2L2); 1265.38 (5%, $FeC_{76}H_{58}N_{10}O_4Cl$, M^{2+} + Cl^-); 1329.36 (3%, $FeC_{76}H_{58}N_{10}O_8Cl$, M^{2+} + ClO_4^-). **FT-IR (KBr):** $\tilde{\nu}$/cm^{-1} = 3135, 3038, 2931, 2866, 1727, 1629, 1581, 1558, 1526, 1496, 1460, 1432, 1410, 1373, 1337, 1258, 1213, 1158, 1094, 1056, 1016, 972, 842, 818, 792, 771, 751, 717, 681, 643, 623, 590, 491.

Synthesis of $[Fe(L2)_2](BF_4)_2\cdot CH_3CN\cdot H_2O$ (3)

A solution of $Fe(BF_4)_2\cdot 6H_2O$ (27.50 mg, 0.082 mmol) in MeOH (3 mL) was added to 98 mg (0.167 mmol) of **L2** dissolved in CH_2Cl_2 (15 mL). Immediately, a colour change from colourless to yellow occurred and the reaction mixture was stirred at room temperature for two hours under a N_2 atmosphere. Solvent was removed by rotary evaporation, the resulting yellow-orange solid was dissolved in CH_3CN and, after diffusion of diethyl ether into this solution, the polycrystalline $[Fe(\mathbf{L2})_2](BF_4)_2\cdot CH_3CN\cdot H_2O$ compound was obtained (64.4 mg, yield 54%). **Elemental analysis found (calcd)** for $C_{78}H_{63}B_2F_8FeN_{11}O_5$ ($[Fe(C_{38}H_{29}O_2N_5)_2](BF_4)_2\cdot CH_3CN\cdot H_2O$, 1463.90 g mol^{-1}): C 63.72 (64.00)%; H 4.28 (4.34)%, N 10.36 (10.52)%. **^{1}H NMR (300 MHz, CD_3CN, 25 °C, δ (ppm)):** 67.00 (s, pyrazole), 58.65 (s, pyrazole), 39.62 (d, pyrazole), 8.27–7.39 (m), 5.70 (s, –C<u>H</u>$_2$–Ph), 3.34 (t, –CH_2–), 2.51 (t, –CH_2–). **ESI-TOF MS** in CH_3CN (Da): *m*/*z* (rel. intensity, assigned structure) = 321.62 (35%, $FeC_{38}H_{29}N_5O_2Cl$, M^{2+} – L2); 615.26 (100%, $FeC_{76}H_{58}N_{10}O_4$, **M^{2+}**, calc. = 615.20); 909.40 (17%, $FeC_{114}H_{87}N_{15}O_6$, M^{2+} + L2); 1203.04 (7%, $FeC_{152}H_{116}N_{20}O_8$, M^{2+} + 2L2). **FT-IR (KBr):** $\tilde{\nu}$/cm^{-1} = 3135, 3038, 2939, 2875, 2250, 1738, 1630, 1583, 1560, 1526, 1497, 1461, 1431, 1410, 1375, 1338, 1257, 1217, 1176, 1160, 1051, 1034, 972, 914, 843, 827, 792, 780, 769, 710, 680, 643, 630, 591, 520, 492.

Caution. *Although we have experienced no difficulties in handling these complexes, metal–organic perchlorates are potentially explosive and should be handled with care and in small quantities.*

Acknowledgements

This research was supported by the DFG Collaborative Research Center TR88 (3MET) under subprojects C5 and C7. We also acknowledge infrastructure support by KIT and the Helmholtz Association.

Notes and references

1 For a general overview on spin-transition compounds, see: (*a*) O. Kahn and C. J. Martinez, *Science*, 1998, **279**, 44; (*b*) P. Gütlich and H. A. Goodwin, *Top. Curr. Chem.*, 2004, **233**; (*c*) E. König, *Prog. Inorg. Chem.*, 1987, **35**, 527; (*d*) E. König, *Struct. Bonding (Berlin)*, 1991, **76**, 51; (*e*) P. Gütlich, Y. Garcia and H. A. Goodwin, *Chem. Soc. Rev.*, 2000, **29**, 419; (*f*) J. A. Real, A. B. Gaspar, V. Niel and M. C. Muñoz, *Coord. Chem. Rev.*, 2003, **236**, 121; (*g*) M. A. Halcrow, *Coord. Chem. Rev.*, 2005, **249**, 2880; (*h*) O. Kahn and J. P. Launay, *Chemtronics*, 1988, **3**, 140.

2 J. M. Holland, J. A. McAllister, C. A. Kilner, M. Thornton-Pet, A. J. Bridgeman and M. A. Halcrow, *J. Chem. Soc., Dalton Trans.*, 2002, 548.

3 J. M. Holland, J. A. McAllister, Z. Lu, C. A. Kilner, M. Thornton-Pett and M. A. Halcrow, *Chem. Commun.*, 2001, 577.

4 M. A. Halcrow, *Polyhedron*, 2007, **26**, 3523.

5 M. A. Halcrow, *Coord. Chem. Rev.*, 2009, **253**, 2493 and references therein.

6 (*a*) C. Rajadurai, O. Fuhr, R. Kruk, M. Ghafari, H. Hahn and M. Ruben, *Chem. Commun.*, 2007, 2636; (*b*) N. T. Madhu, I. Šalitroš, F. Schramm, S. Klyatskaya, O. Fuhr and M. Ruben, *C. R. Chim.*, 2008, **11**, 1166 and references therein; (*c*) I. Šalitroš, N. T. Madhu, R. Boca, J. Pavlik and M. Ruben, *Monatsh. Chem.*, 2009, **140**, 695.

7 (*a*) M. Cavallini, I. Bergenti, S. Milita, G. Ruani, I. Salitros, Z.-R. Qu, R. Chandrasekar and M. Ruben, *Angew. Chem., Int. Ed.*, 2008, **47**, 8596; (*b*) S. Cobo, G. Molnár, J. A. Real and A. Bousseksou, *Angew. Chem., Int. Ed.*, 2006, **45**, 5786; (*c*) G. Molnár, S. Cobo, J. A. Real, F. Carcenac, E. Daran, C. Vieu and A. Bousseksou, *Adv. Mater.*, 2007, **19**, 2163; (*d*) C. Thibault, G. Molnár, L. Salmon, A. Bousseksou and C. Vieu, *Langmuir*, 2010, **26**, 1557.

8 S. Klyatskaya, J. R. Galán Mascarós, L. Bogani, F. Hennrich, M. Kappes, W. Wernsdorfer and M. Ruben, *J. Am. Chem. Soc.*, 2009, **131**, 15143.

9 (*a*) O. Kahn, J. Kröber and C. Jay, *Adv. Mater.*, 1992, **4**, 718; (*b*) N. Moliner, M. C. Muñoz, S. Letard, X. Solans, N. Menéndez, A. Goujon, F. Varret and J. A. Real, *Inorg. Chem.*, 2000, **39**, 5390; (*c*) V. Niel, J. M. Martinez-Agudo, M. C. Muñoz, A. B Gaspar and J. A. Real, *Inorg. Chem.*, 2001, **40**, 3838; (*d*) A. Galet, V. Niel, M. C. Muñoz and J. A. Real, *J. Am. Chem. Soc.*, 2003, **125**, 14224; (*e*) J. A. Real, E. Andrés, M.

C. Muñoz, M. Julve, T. Granier, A. Bousseksou and F. Varret, *Science*, 1995, **268**, 265; (*f*) D. L. Reger, J. R. Gardinier, M. D. Smith, A. M. Shahin, G. J. Long, L. Rebbouh and F. Grandjean, *Inorg. Chem.*, 2005, **44**, 1852.

10 (*a*) M. Ruben, F. J. Rojo, J. Romero-Salguero and J. M. Lehn, *Angew. Chem., Int. Ed.*, 2004, **43**, 3644; (*b*) E. Breuning, M. Ruben, J. M. Lehn, F. Renz, Y. Garcia, V. Ksenofontov, P. Gütlich, E. Wegelius and K. Rissanen, *Angew. Chem., Int. Ed.*, 2000, **39**, 2504; (*c*) T. Kitazawa, Y. Gomi, M. Takahashi, M. Takeda, M. Enomoto, A. Miyazaki and T. Enoki, *J. Mater. Chem.*, 1996, **6**, 119; (*d*) V. Niel, A. L. Thompson, A. E. Goeta, C. Enachescu, A. Hauser, A. Galet, M. C. Muñoz and J. A. Real, *Chem.–Eur. J.*, 2005, **11**, 2047; (*e*) A. Galet, M. C. Muñoz, V. Martínez and J. A. Real, *Chem. Commun.*, 2004, 2268; (*f*) V. Niel, M. C. Muñoz, A. B. Gaspar, A. Galet, G. Levchenko and J. A. Real, *Chem.–Eur. J.*, 2002, **8**, 2446.

11 (*a*) R. Boča, M. Boča, L. Dlháň, K. Falk, H. Fuess, W. Haase, R. Jaroščiak, B. Papánková, F. Renz, M. Vrbová and R. Werner, *Inorg. Chem.*, 2001, **40**, 3025; (*b*) S. Hayami, Z. Gu, H. Yoshiki, A. Fujishima and O. Sato, *J. Am. Chem. Soc.*, 2001, **123**, 11644; (*c*) Y. Garcia, G. Bravic, C. Gieck, D. Chasseau, W. Tremel and P. Gütlich, *Inorg. Chem.*, 2005, **44**, 9723.

12 C. Rajadurai, F. Schramm, S. Brink, O. Fuhr, M. Ghafari, R. Kruk and M. Ruben, *Inorg. Chem.*, 2006, **45**, 10019.

13 C. A. Tovee, C. A. Kilner, S. A. Barrett, J. A. Thomas and M. A. Halcrow, *Eur. J. Inorg. Chem.*, 2010, 1007.

14 L. Salmon, G. Molnár, D. Zitouni, C. Quintero, C. Bergaud, J. C. Micheau and A. Bousseksou, *J. Mater. Chem.*, 2010, **20**, 5499.

15 J. R. Lakowicz, in *Principles of Fluorescence Spectroscopy*, Kluwer Academic/Plenum Publishers, New York, 1999, Chapter 3, and references therein.

16 G. M. Sheldrick, *Acta Crystallogr., Sect. A*, 2008, **64**, 112.

17 (*a*) M. Ruben, A. Landa, E. Lörtscher, H. Riel, M. Mayor, H. Görls, H. B. Weber, A. Arnold and F. Evers, *Small*, 2008, **4**, 2229; (*b*) E. A. Osorio, T. Bjornholm, J. M. Lehn, M. Ruben and H. S. J. Van Der Zant, *J. Phys.: Condens. Matter*, 2008, **20**, 374121.

18 (*a*) N. Lin, S. Stepanov, F. Vidal, K. Kern, M. S. Alam, S. Strömsdörfer, V. Dremov, P. Müller, A. Landa and M. Ruben, *Dalton Trans.*, 2006, 2794; (*b*) M. Ruben, *Angew. Chem., Int. Ed.*, 2005, **44**, 1594.